Electronic Supplementary Material (ESI) for Physical Chemistry Chemical Physics.

Supporting Information for

CO_2 Hydrogenation to Methanol over In-doped m-ZrO_2: A DFT Investigation into the Size-Dependent Mechanism of Oxygen Vacancy

Jie Yu,[a] Yabing Zeng,[b] Wei Lin,[*b,c] and Xin Lu[*a,c]

[a] *State Key Laboratory of Physical Chemistry of Solid Surfaces, College of Chemistry and Chemical Engineering, Xiamen University, Xiamen 361005, Fujian, China.*

[b] *College of Chemistry, Fuzhou University, Fuzhou 350108, Fujian, China.*

[c] *Fujian Provincial Key Laboratory of Theoretical and Computational Chemistry, Xiamen University, Xiamen 361005, Fujian, China.*

* Corresponding authors.

Tel: +86-0592-2181600; Fax: +86-0592-2183047.

E-mail: xinlu@xmu.edu.cn (Xin Lu); wlin@fzu.edu.cn (Wei Lin).

Table S1. Surface Formation Energies of (111) m-ZrO_2

Exposed Phase	γ/(J.m^2) for relaxed surface				γ/(J.m^2) for unrelaxed surface			
	This work	PBE[1]	PW91[2]	LDA[3]	This work	PBE	PW91	LDA
(111)	1.11	1.11	1.06	1.54	1.42	1.39	1.39	1.86

Table S2. Oxygen Vacancy Formation Energy ($E_{(vac)}$, in eV) of ZrO_2_T2, ZrO_2_T3 and ZrO_2_T4 by thermal, H_2 and CO reductions.

reduction type	surface model	a	b	c	d	e
thermal reduction	ZrO_2_T2	5.81	6.43	5.59	6.40	6.76
	ZrO_2_T3		6.76	5.76	6.23	5.59
	ZrO2_T4	5.97	5.13	6.17	5.41	5.64
H_2 reduction	ZrO_2_T2	3.26	2.79	3.10	3.46	2.88
	ZrO_2_T3		4.22	3.23	3.69	3.05
	ZrO2_T4	3.43	2.60	3.63	2.87	3.1
CO reduction	ZrO_2_T2	2.53	2.06	2.37	2.73	2.15
	ZrO_2_T3		3.50	2.50	2.96	2.32
	ZrO2_T4	2.71	1.87	2.91	2.15	2.37

Table S3. Calculated bond distances (in Å) between specific atoms of perfect and O_v defective In@m-ZrO_2 surfaces.

	Zr1-In	Zr5-In	Zr1-Zr5	Zr3-In	Zr4-In	Zr3-Zr5
perfect In@m-ZrO_2	3.55	3.44	3.48	3.99	3.47	3.64
O1_v defective In@m-ZrO_2	3.79	3.69	3.86	3.91	3.51	3.63
O2_v defective In@m-ZrO_2	3.86	3.50	3.53	3.87	3.42	3.67
O4_v defective In@m-ZrO_2	3.43	3.45	3.44	4.32	4.14	4.68

Table S4. Reaction energies (in eV) of atomic hydrogen migration on the O1_v, O2_v and O4_v surfaces.

	ΔE					
	O4	O6	O8	O9	O10	O11
Homo-transfer[a]			**O1_v**			
	0.31	0.81	0.61	0.33	0.47	0.37
			O2_v			
	0.66	0.59	0.35	0.02	0.17	0.07
			O4_v			
		0.49	0.78	0.49	0.92	0.22
Heterogenous-transfer[b]			**O1_v**			
	0.29	0.34	0.42	0.25	0.37	0.24
			O2_v			
	0.23	0.32	0.41	0.21	0.36	0.24
			O4_v			
		0.46	0.67	0.57	0.79	0.37

a. Homo-transfer is defined as fixing one of the dissociative hydrogen atoms at O7 while migration the other to O6-O10 individually.

b. Heterogenous-transfer is defined as fixing one of the dissociative hydrogen atoms at In while migration the other to O6-O10 individually.

Table S5. Calculated Harmonic Vibrational Frequencies (cm^{-1}) of stable-CH_3O (s-CH_3O) on O1_v and O4_v surface

s-CH_3O* on O1_v	**s-CH_3O* on O4_v**
3047	3043
3025	3017
2941	2937
1471	1473
1453	1461
1430	1429
1171	1174
1140	1137
1035[a]	1000[b]
412	334
259	281
221	202
175	143
153	137
93	110

a. Frequency of C-O stretching mode for s-CH_3O* on O1_v

b. Frequency of C-O stretching mode for s-CH_3O* on O4_v

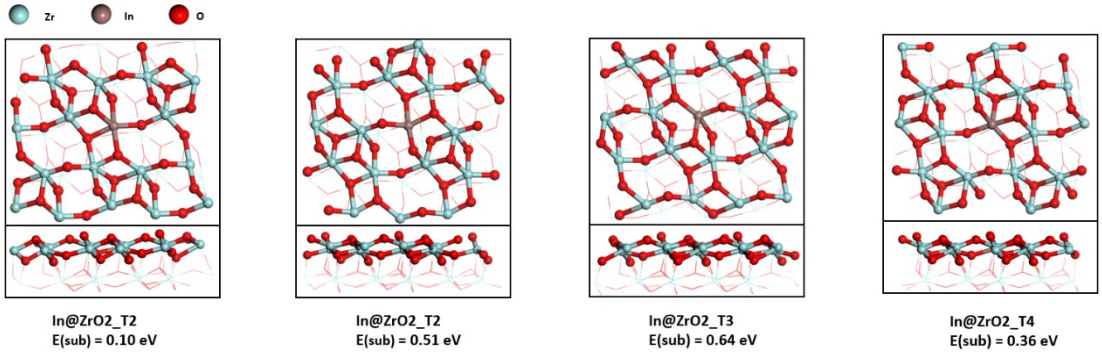

Figure S1. Optimized structures of In@m-ZrO_2_T1 to In@m-ZrO_2_T4 surfaces top (upper) and side (lower) view and their respective In substitution energy ($E_{(sub)}$)

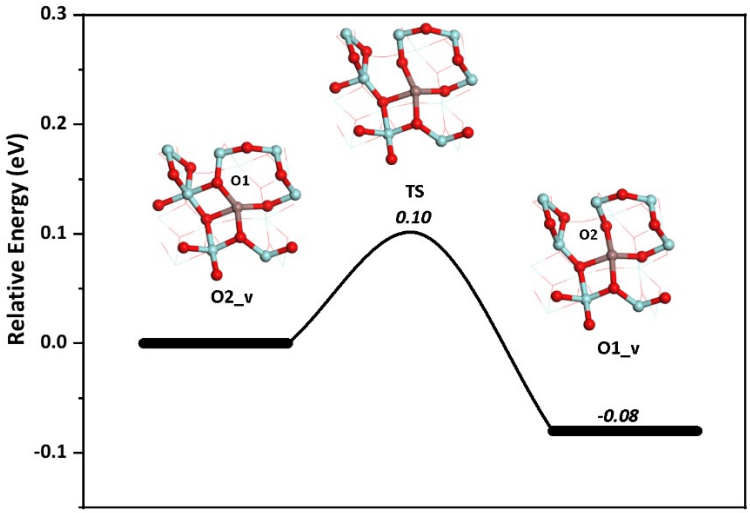

Figure S2. Potential energy diagram of dynamic equilibrium between O1_v and O2_v defective In@m-ZrO_2.

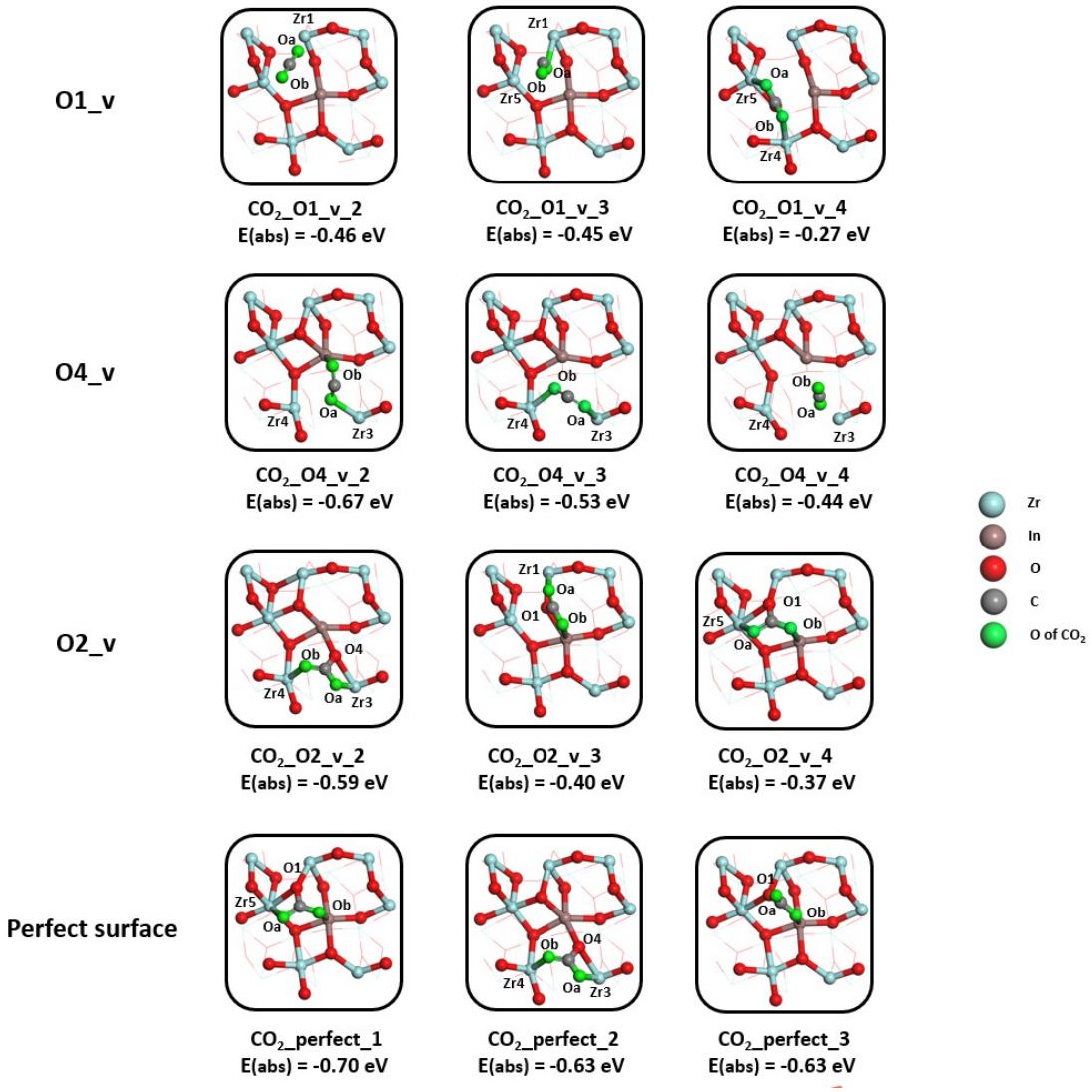

Figure S3. Other optimized structures of CO_2 adsorption on O1_v defective In@m-ZrO_2, O4_v defective In@m-ZrO_2, O2_v defective In@m-ZrO_2 and perfect In@m-ZrO_2.

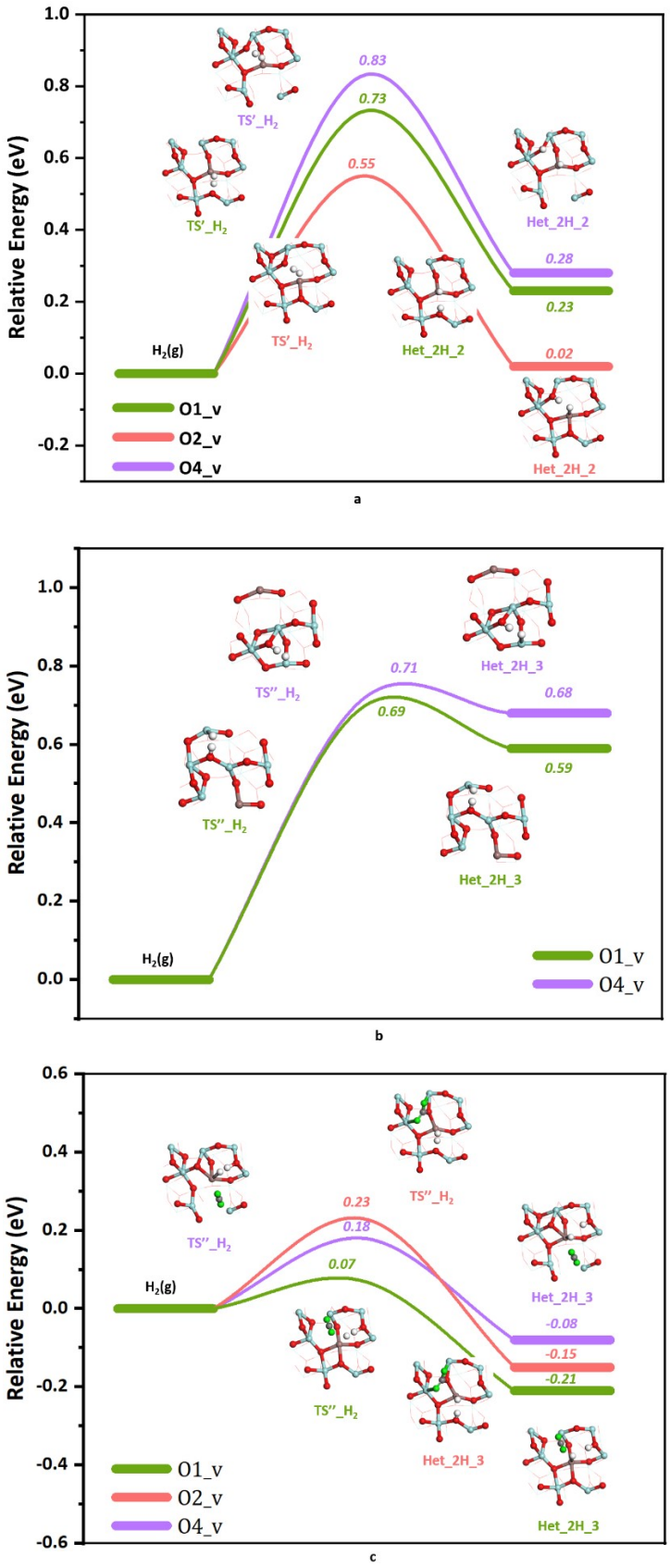

Figure S4. Potential energy diagram of (a) less favorable H_2 heterolytic dissociation between In and O on O1_v (green), O4_v (purple) and O2_v (pink) surfaces; (b) H_2 heterolytic dissociation

between Zr and O on O1_v (green) and O4_v (purple); (c) H_2 heterolysis dissociation between In and O on O1_v (green), O2_v (red) and O4_v (purple) in the presence of CO_2 adsorption.

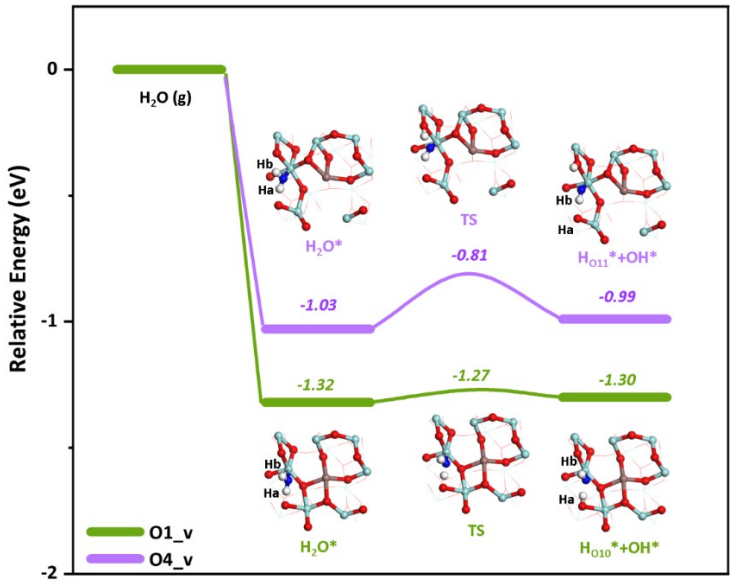

Figure S5. Potential energy diagram of H_2O dissociation on O1_v (green) and O4_v (purple) surfaces. Atoms in blue color represents oxygen atom from dissociated H_2O.

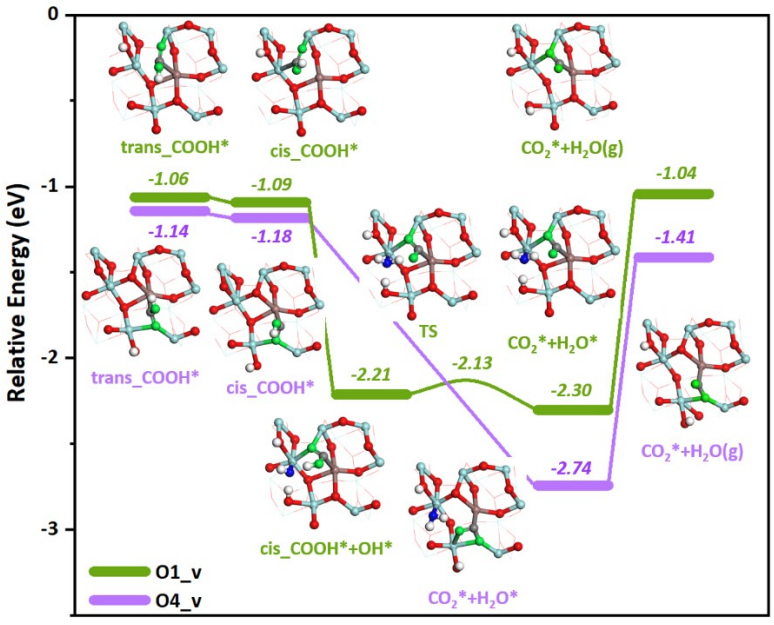

Figure S6. Potential energy diagram of OH* assisted deprotonation of COOH on O1_v (green) and O4_v (purple) surfaces. Atom in blue and green colors represents oxygen atoms from H_2O and CO_2, respectively.

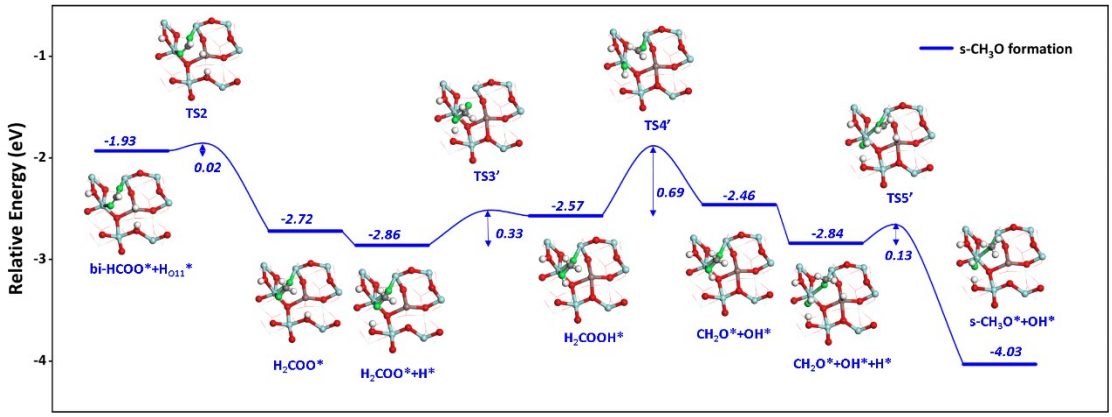

Figure S7. Potential energy diagram of stable-CH_3O(s-CH_3O) formation on O1_v surface.

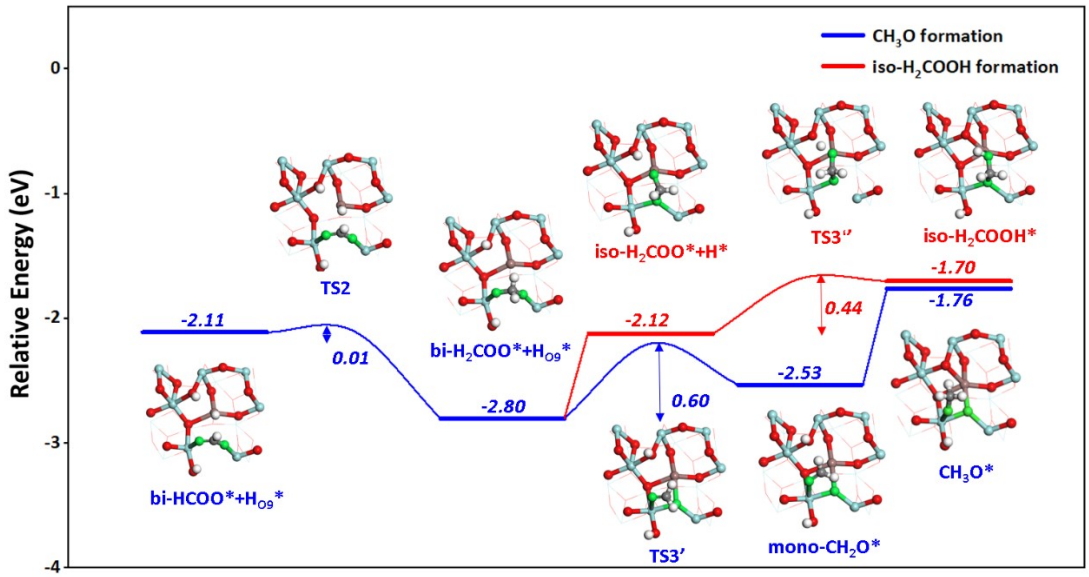

Figure S8. Potential energy diagram of other reactions during CO_2 hydrogenation on O4_v surface.

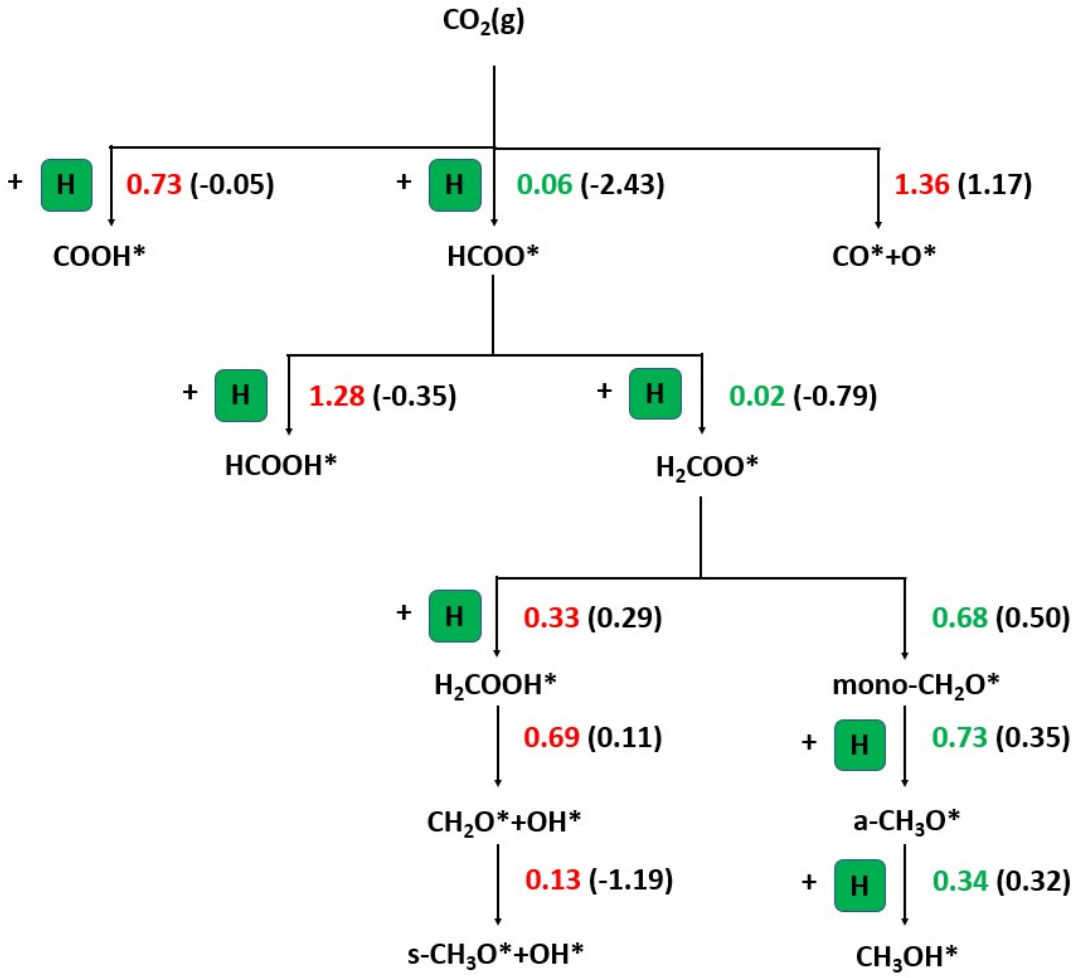

Figure S9. Reaction network of CO_2 hydrogenation on O1_v defective In@m-ZrO_2. The reaction barrier is marked with number in either green (the most preferred route leading to methanol synthesis) or red (other routes). The reaction energy is marked with black number in the bracket. Unit of relative energy are given in electronic voltage (eV).

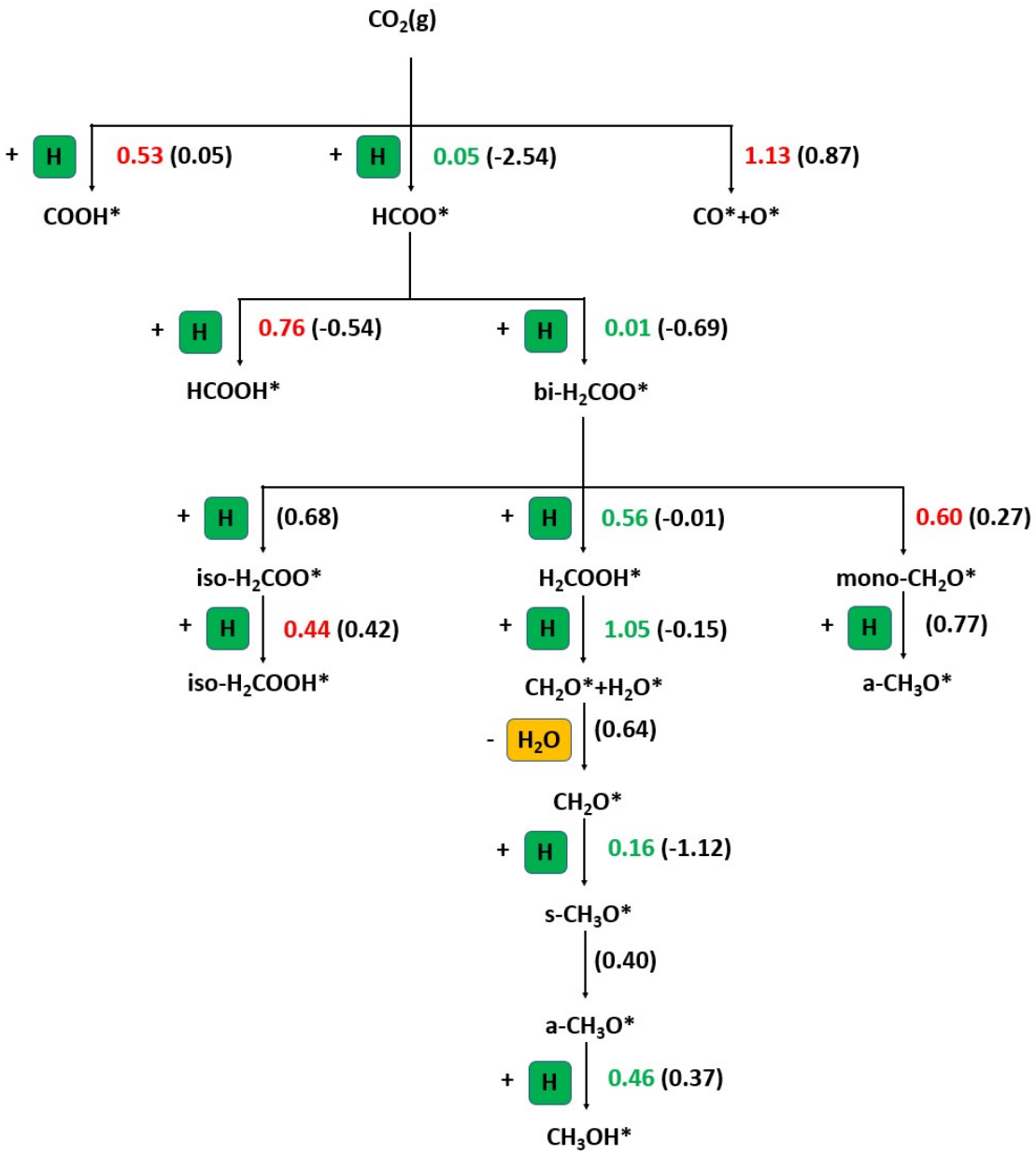

Figure S10. Reaction network of CO_2 hydrogenation on O4_v defective In@m-ZrO_2. The reaction barrier is marked with number in either green (the most preferred route leading to methanol synthesis) or red (other routes). The reaction energy is marked with black number in the bracket. Unit of relative energy are given in electronic voltage (eV).